Facile Synthesis of Bimetallic CuS - Ag/ZnO Nanoparticles By Hydrothermal Method and Its Application as Photocatalytic Degradation of Methylene Blue

Ezza Zulfiqar

SCOPUA BOOKS

Facile Synthesis of Bimetallic CuS-Ag/ZnO Nanoparticles by Hydrothermal Method and Its Application as Photocatalytic Degradation of Methylene Blue

By

Ezza Zulfiqar

Series Title: SCOPUA Books

Scientific Collaborative Online Publishing Universal Academy

Book Title

Facile Synthesis of Bimetallic CuS- Ag/ZnO Nanoparticles by Hydrothermal Method and Its Application as Photocatalytic Degradation of Methylene Blue

Series Name

SCOPUA Books

Author(s)

Ezza Zulfiqar

Centre for Applied Chemistry, Institute of Chemistry, Punjab University Lahore, Pakistan

*Corresponding: ezzazulfiqar14@gmail.com

Published On

August 21, 2025 (Edition 1)

Publisher

Scientific Collaborative Online Publishing Universal Academy, Lahore, Pakistan

Contact / Email

editor@books.scopua.com

ISBN: 978-627-7898-07-6

DOI: 10.64060/978-627-7898-07-6

BISAC

SCI013010, SCI013000

THAMA

PNF, PN

Abstract

The current research study was performed to synthesize the bimetallic Ag/ZnO nanoparticles using CuS as a coating material and to study its application as a photocatalytic degradation of Methylene blue. MB poses a great threat to human life as well as to aquatic life if present in water. Therefore, in this study, we design an economical method to degrade this dangerous dye. The bimetallics were synthesized via the hydrothermal method, which is a very cheap method and has proved very efficient. The dye was degraded by varying different factors such as the concentration of the catalyst and the time factor. The results were examined by UV and FT-IR. This study proposed the best result for degrading dyes from the environment.

Dedication

All praise to Allah Almighty, the most Beneficial and the Merciful, who always showers his blessings upon me and enables me to gain knowledge in my research work. Without his grace and mercy, this work would not have been accomplished. All respect to Prophet Muhammad (P.B.U.H) for a unique, comprehensive, and everlasting source of guidance and knowledge for humanity.

My dedication goes to my teachers for their patience and guidance during my studies. My most sincere thanks go to my family, especially my mother and grandfather, for their support. I am also thankful to the SCOPUA Books for their support in publishing this work as a book.

Acknowledgements

I am thankful to my supervisor Dr. Zaib-un-Nisa Hussain, Director, Centre for Applied Chemistry, Institute of Chemistry, Punjab University Lahore for her continuous encouragement and generous support throughout my work. Thank you for guiding me in every aspect of my research work. I would like to pay my gracious thanks to my respected, sincere, kind and highly qualified co-supervisor Dr. Imran Din. His support, tolerance and guidance helped me overcome numerous difficulties in research.

This book project did not receive any specific grant from funding agencies in the public, commercial, or not-for-profit sectors. The author declares that she has no known competing financial interests or personal relationships that could have appeared to influence the work reported in this book. I hereby declare that the work reported in this book was derived from my master's thesis, submitted by me based on my research work.

Table of Content

CHAPTER ONE

INTRODUCTION TO THE RESEARCH

Ezza Zulfiqar

Centre for Applied Chemistry, Institute of Chemistry, Punjab University Lahore, Pakistan

***Corresponding: ezzazulfiqar14@gmail.com**

1. INTRODUCTION

This chapter reviews the self-assembly of nanoparticles into two-dimensional structure and has developed the promising strategy to formulate the efficient catalyst and photo catalysts for the purification of water. It is a big challenge of organic pollutants in dyeing industry in the world with the fast development of industrial technology in the past half century[1]. With the increase in industrialization [1, 2], direct discharge of harmful chemicals into the environment [3] has also increased to a greater extent. In recent information, more than 100 thousand commercially dye products have discharged to the aquatic environment [4] [5]. Textile industries were the largest contributor to water pollution followed by paint, paper, leather, and printing industries [6, 7]. Disposal of dye into environment is harmful to the aquatic life ecosystem and posed negative impact to human health. The consequences can be in the form of aesthetic disorders, such as discoloration and foul-smelling water and life disruption of water ecosystems due to reduction of sunlight penetration and depletion of oxygen level in water. The risk of dye pollution in water for human health includes the emergence of skin diseases upon contact with polluted water and digestive disorders from water consumption that may lead that may lead to the potential risk of cancer [8, 9].Thus, the degradation of dyes must be compulsory from the environment. For this, nanotechnology has become a useful technique applied these days. In this study, the photocatalytic degradation of MB has been done efficiently using bimetallic Ag-ZnO NPs.

1.1 Dyes

A **dye** is a colored substance that chemically bonds to the substrate to which it is being applied. This distinguishes

dyes from pigments which do not chemically bind to the material they color. Dye is generally applied in an aqueous solution, and may require a mordant to improve the fastness of the dye on the fiber. The majority of natural dyes are derived from other sources : roots, berries, bark, leaves, wood, fungi and lichens[10]. In the 21st century, most dyes are synthetic, i.e., are man-made from petrochemicals. The color of a dye is dependent upon the ability of the substance to absorb light within the visible region of the electromagnetic spectrum (380-750 nm). An earlier theory known as Witt theory stated that a colored dye had two components, a chromophore which imparts color by absorbing light in the visible region (some examples are nitro, azo, quinoid groups) and an auxochrome which serves to deepen the color. This theory has been superseded by modern electronic structure theory which states that the color in dyes is due to excitation of valence π-electrons by visible light [11].

1.1.2. Types of Dyes

Dyes are classified according to their solubility and chemical properties [12].

Acid dyes are water-soluble anionic dyes that are applied to fibers such as silk, wool, nylon and modified acrylic fibers using neutral to acid dye baths. Attachment to the fiber is attributed, at least partly, to salt formation between anionic groups in the dyes and cationic groups in the fiber. Acid dyes are not substantive to cellulosic fibers. Most synthetic food colors fall in this category. Examples of acid dye are Alizarin Pure Blue B, Acid red 88, etc.

Basic dyes are water-soluble cationic dyes that are mainly applied to acrylic fibers, but find some use for wool and silk. Usually acetic acid is added to the dye bath to help the uptake

of the dye onto the fiber. Basic dyes are also used in the coloration of paper.

Mordant dyes require a mordant, which improves the fastness of the dye against water, light and perspiration. The choice of mordant is very important as different mordents can change the final color significantly. Most natural dyes are mordant dyes and there is therefore a large literature base describing dyeing techniques. The most important mordant dyes are the synthetic mordant dyes, or chrome dyes, used for wool; these comprise some 30% of dyes used for wool, and are especially useful for black and navy shades.

Vat dyes are essentially insoluble in water and incapable of dyeing fibers directly. However, reduction in alkaline liquor produces the water-soluble alkali metal salt of the dye. This form is often colorless, in which case it is referred to as a Leuco dye, and has an affinity for the textile fiber. Subsequent oxidation reforms the original insoluble dye. The color of denim is due to indigo, the original vat dye.

Reactive dyes utilize a chromophore attached to a substituent that is capable of directly reacting with the fiber substrate. The covalent bonds that attach reactive dye to natural fibers make them among the most permanent of dyes. "Cold" reactive dyes, such as Procion MX, Cibacron F, and Drimarene K, are very easy to use because the dye can be applied at room temperature. Reactive dyes are by far the best choice for dyeing cotton and other cellulose fibers at home or in the art studio.

Disperse dyes were originally developed for the dyeing of cellulose acetate, and are water-insoluble. The dyes are finely ground in the presence of a dispersing agent and sold as a paste, or spray-dried and sold as a powder. Their main use is

to dye polyester, but they can also be used to dye nylon, cellulose triacetate, and acrylic fibers. In some cases, a dyeing temperature of 130 °C (266 °F) is required, and a pressurized dyebath is used. The very fine particle size gives a large surface area that aids dissolution to allow uptake by the fiber. The dyeing rate can be significantly influenced by the choice of dispersing agent used during the grinding.

Sulfur dyes are inexpensive dyes used to dye cotton with dark colors. Dyeing is effected by heating the fabric in a solution of an organic compound, typically a nitrophenol derivative, and sulfide or polysulfide. The organic compound reacts with the sulfide source to form dark colors that adhere to the fabric. Sulfur Black 1, the largest selling dye by volume, does not have a well-defined chemical structure.

2. METHLENE BLUE

Methylthioninium chloride, commonly called **methylene blue**, is a salt used as a dye and as a medication. Methylene blue is a thiazine dye [13]. It works by converting the ferric iron in hemoglobin to ferrous iron. As a medication, it is mainly used to treat methemoglobinemia. Specifically, it is used to treat methemoglobin levels that are greater than 30% or in which there are symptoms despite oxygen therapy. It has previously been used for cyanide poisoning and urinary tract infections, but this use is no longer recommended. The side effects of MB are given in the Table 1;

Cardiovascular	Central Nervous System	Dermatologic	Gastrointestinal	Genito-urinary	Hematologic
• Hypertension • Precordial pain	• Dizziness • Mental	Staining of skin • Injection	• Fecal discoloration • Nausea	• Discoloration of urine (dos	• Anemia

	confusion • Head ache • Fever	site necrosis (SC)	• Vomiting • Abdominal pain	es over 80 µg) • Bladder irritation	

Table 1: *Side Effects of MB*

The structure of MB is shown as follow in Figure 1.

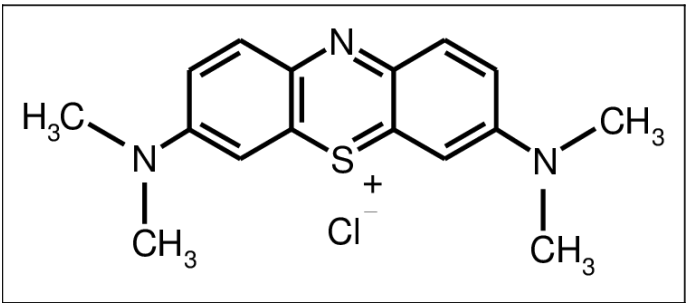

Figure 1: *Structure of MB*

MB is mainly used to dye paper and office supplies, but also used to tone up silk colors, as stain in microscopy, used in industries for coloring paper, cotton, silk, wool and for hair coloring and reported to cause several risks to human health, such as eye, respiratory, digestive and mental disorders [14, 15]. Removal of MB from industrial waste has been investigated using various methods such as enzymatic process, photo degradation reaction, electrochemical removal, chemical coagulation, membrane filtration and physical adsorption methods [15]. However, these methods cannot remove pollutants thoroughly. Oxidation is an alternative treatment strategy that can be applied to dyes and many other organics in wastewater and industrial effluents. In particular, semiconductor mediated photocatalytic oxidation can be conveniently applied towards the degradation of dye pollutants.

3. PHOTOCTALYTIC DEGRADATION

Photocatalytic degradation of organic pollutants is promising technology due to its advantage of degradation on pollutants instead of their transformation under ambient conditions. In chemistry, photo catalysis is the acceleration of a photoreaction in the presence of a catalyst. In catalyzed photolysis, light is absorbed by an adsorbed substrate. Photocatalytic degradation of organic pollutants in water and air using semi conductive particles, such as TiO2 and ZnO, has attracted extensive attention in the past two decades [16, 17]. In particular, ZnO has attracted much attention with respect to the degradation of various pollutants due to its high photosensitivity, stability and wide band. While TiO2 is widely employed as a photo catalyst, ZnO is a suitable alternative to TiO2 as it has a similar band gap energy (3.2 eV) [18] larger quantum efficiency than TiO2 and higher photocatalytic efficiencies have been reported [19, 20] gap. The following Figure 2 shows the photocatalytic degradation mechanism.

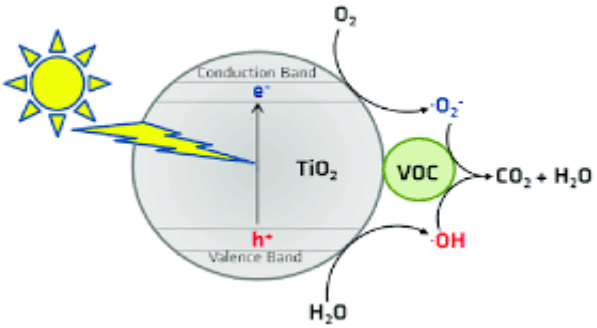

Figure 2: *Mechanism of photocatalytic degradation*

4. NONTECHNOLOGY

Nanotechnology is becoming important in enabling advances of new and effective techniques both to synthesize and characterize materials and devices at the Nano-scale, as well as

the possibilities that such technology offers to substantially expand the attainable limits in many different fields including medicine, electronics, chemistry, and engineering[21]. It is a creation of functional materials, devices, and systems through the manipulation of matter in nanodomain. Nanotechnology has extensive and prevalent interest in many fields is ascribed to the phenomenally enhanced crystallographic characteristics of the nanostructures due to their very small size [22]. Due to their applications in heterogeneous catalysis, they are becoming a matter of interest with time [23].

5. NANOPARTICLES

Nanoparticles (NPs) are of particular interest among all nanomaterial owing to their characteristic features and vast applications. Nanoparticles are actually surface-active Plasmon-resonant colloidal particles having size 1-100 nm [24]. Owing to size in nanometer nanoparticles possess large surface to volume ratio. Nanoparticles have ability of quantum confinement of light [25]. Nanoparticles are optically and electromagnetically active substances due to the existence of a strong coupling between electromagnetic radiations and electron Plasmon of material giving rise to phenomena of Surface Plasmon Resonance (SPR). Nanoparticles are of many types like organic nanoparticles, inorganic nanoparticles, metallic nanoparticles, oxide nanoparticles, semiconductor nanoparticles etc. For Nanoparticle synthesis two methods are utilized i.e. top-down approach and bottom-up approach (Figure 3). Top down approach is the physical/dispersion method which involves the conversion of big molecules into the smaller particle having a size in the nanometer range and bottom- up approach also called chemical/aggregation method by which smaller particles aggregate to form nano range sized

particles [26]. Nanoparticles have vast applications in many fields like drug delivery/carrier systems, bio sensing materials, clinical translation systems, photo catalyst substance and nanoreactor medium.

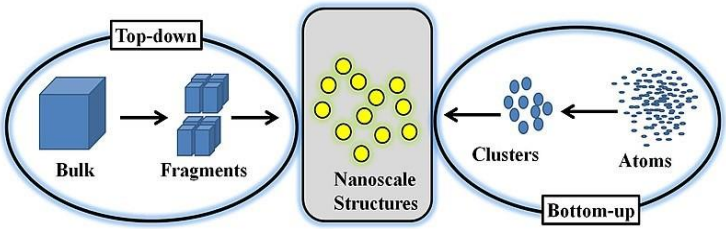

Figure 3: *Top down and bottom up method*

5.1. Nature of Nanoparticles

Silver Nanoparticles: Silver nanoparticles (AgNPs) are one of the most vital and fascinating nanomaterials among several metallic nanoparticles that are involved in biomedical applications. AgNPs play an important role in nanoscience and nanotechnology, particularly in nanomedicine. Although several noble metals have been used for various purposes, AgNPs have been focused on potential applications in cancer diagnosis and therapy. Silver nanoparticles (Ag NPs) with their extraordinary optical properties have become the subject of interest in the field of research. Silver nanoparticles are non-toxic or having low toxicity so it is eco-friendly and can be applied in green chemistry approach [27]. Additionally silver nanoparticles are the only nanomaterial which surface Plasmon resonance wavelength can be manipulated in the visible region of the electromagnetic spectrum and also its Plasmon excitation efficiency is highest among all other NPs [28].Ag NPs are ecofriendly and less costly compared to other MNPs .Therefore, Ag NPs containing suitable stabilizing agent have gained much attention as potential catalysts for the

photocatalytic degradation of MB. Chemical reduction method is the common method for synthesis of AgNPs by using organic and inorganic compounds as reducing agents. Usually, different reducing agents like sodium borohydride (NaBH4), trisodium citrate, polyol process, N, N dimethylformamide (DMF), sodium borohydride (NaBH4), polyethylene glycol-block polymers and Tollens reagent are basically utilized for the reduction of silver ions (Ag+) as reducing agents in the aqueous solutions.

Gold Nanoparticle: Owing to the prominent chemical and physical properties [29] Au nanoparticles have gained a lot of importance and are research hotspot these days. For transformation reactions, Au nanoparticles possess some unique features like high surface area to volume ratio, selectivity [30], stability and thus contributes to wide range of catalytic applications. Examples of catalysis by Au nanoparticles include low temperature oxidation [31] of carbon monoxide, degradation MB as well as the oxidation of alcohols. They are prepared from gold salt and converted from Au ions to Au nanoparticles using glycerol [32] or usually NaBH4. The recovery and recycling of Au nanoparticles can be made possible by supporting them on magnetic materials using magnetic separation [33] approach. On chitosan-coated iron oxide nanoparticles, using the adsorption - reduction of Au (III) ions magnetically recoverable Au nanoparticles were synthesized as reported by researchers. Then its catalytic activity for converting 4-MB into CO_2 and H_2O was studied as model reaction. The only obstruction in usage of Au nanoparticles in catalysis is the fact that they are expensive; their synthesis is not cheap but causes cost.

Zinc Oxide Nanoparticles: Zinc oxide (ZnO) is a type of semiconductor having a broad direct band gap width (3.37 eV), large excitation binding energy (60 meV) and deep violet/borderline ultraviolet (UV) absorption at room temperature[34]. It is an excellent semiconductor oxide that possesses favorable excellent electrical, mechanical and optical properties [35], similar toTiO2. In addition, ZnO not only has antifouling and antibacterial properties, but also good photocatalytic activity [36]. Furthermore, as reported by Liang et al. [37], the production cost of ZnO is up to 75%lower than that of TiO2and Al2O3 nanoparticles. Due to the advantages of ZnO over TiO2, ZnO has been suggested to be used in heterogeneous photo catalysis. According to Herrmann et al. [38], the heterogeneous photocatalytic oxidation steps can be explained as shown in Figure 4.

1. Organic pollutants diffuse from the liquid phase to the surface of ZnO.
2. Adsorption of the organic pollutants on the surface of ZnO.
3. Oxidation and reduction reactions in the adsorbed phase.
4. Desorption of the products.
5. Removal of the products from interface region.

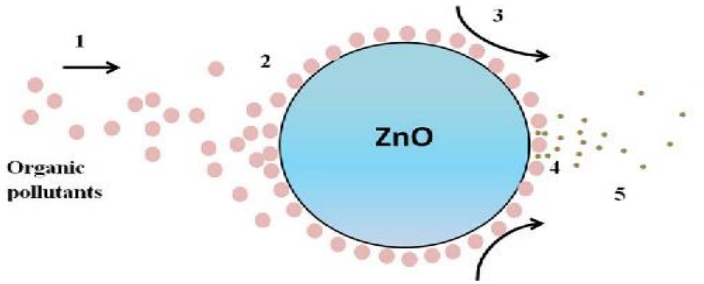

***Figure 4**: Heterogeneous photocatalytic oxidation steps.[38]*

Copper Nanoparticles: Copper nanoparticles(CuNPs) have attracted more attention because of their catalytic, optical, electrical and antifungal/antibacterial applications [39]. Besides, copper is an inexpensive and available element; it shows less electro migration influence when it is applied in microelectronics, compared with other noble metals [40]. These different applications originated from the unique chemical and physical properties that copper nanoparticles have [40]. Hence, various physical and chemical synthetic routes have been reported for the fabrication of copper nanoparticles (CuNPs) including micro emulsion, thermal decomposition, aqueous chemical reduction, laser ablation, vapor decomposition, precipitation, sol-gel, electrospinning, electrochemical, and microwave-assisted methods [41, 42]. Nevertheless, fabrication of stable and pure CuNPs is still a challenging process because they are more susceptible to oxidation, compared with gold and silver nanostructures [43].

5.2. Bimetallic nanoparticles as Catalysts

Bimetallic nanoparticles (BNPs) have gained a lot of importance now as they possess some basic important features as increased physical properties as surface morphology [44], shape and size. As they are made up of two different metals, so their potential is increased synergistically. They are more efficient and superior over monometallic nanoparticles because the drawback of one is overcome by another present. So, within one assembly we get the traits of both the metals. So better selectivity, catalytic properties and long-lasting stability is obtained by using bimetallic nanoparticles. These bimetallic nanoparticles can also be reused and can be separated from reaction mixture. BNPs show specific properties that are

different from those of the corresponding individual metal nanoparticles. In other words, they could illustrate better activity compared to their monometallic counterparts (synergistic effects). BNPs can be arranged in random alloy, core–shell or cluster-in-cluster structures [45, 46]. Generally, they could be obtained either by co-reduction, or subsequent reduction [47]. The preparation methods and conditions strongly influence the structure, size and composition of BNPs [48].

Ag-ZnO Bimetallic Nanoparticles: The metal-semiconductor nanostructure has been already considered to be a photocatalyst with great potential for environmental purification in the future due to the special interface interaction. Unlike Pt, Pd and Au, Ag possesses many advantages such as high efficiency, low cost and easy preparation [49], which was deposed on the surfaces of various ZnO nanostructures, giving rise to excellent photocatalytic properties. For one thing, Ag deposed on ZnO surface can not only function as a co-catalyst for the promotion of redox reactions, but also a light-harvesting antenna for enhancing visible light absorption [50]. For another thing, Ag loading can inhibit the photocatalytic reaction-induced corrosion and photo corrosion, and thus enhance the stability of catalyst [51] . So far, many methods such as sol-gel process [52], hydrothermal method [53], photo reduction [54], thermal reduction [55], biogenic reduction [30], have been applied to synthesize Ag-ZnO nanophotocatalysts. In this project, the Ag-ZnO NPs are synthesized by hydrothermal method which were used as highly efficient material for photocatalytic degradation of MB and biological process.

6. Aims and Objective of the study

Here, we present the novel synthesis of Ag-ZnO/ CuO bimetallic nanoparticles by hydrothermal method. Following are the main objectives of this study:

- Synthesis of Ag ZnO bimetallic photocatalyst using CuSO4 as base material.
- Characterization of CuO and Ag-ZnO bimetallic with the help of UV- visible and FT-IR spectroscopy.
- Report of photocatalytic action of Ag-ZnO NPs for the degradation of MB into H2O and CO_2 with the help of UV-visible spectroscopy.
- Studying different parameters that effects the degradation rate of MB in the presence of sun light.

CHAPTER TWO

LITERATURE REVIEW

Ezza Zulfiqar

Centre for Applied Chemistry, Institute of Chemistry, Punjab University Lahore, Pakistan

***Corresponding: ezzazulfiqar14@gmail.com**

Ahmad et al., [56] reported the synthesis of Cu-doped ZnO nanoparticles embedded on multi walled carbon nanotubes (CNTs) having light responsive by sol method. They characterized the catalytic activities of photocatalyst using SEM, EDX, XRD, HR-TEM, TEM, XPS, BET, and by UV-Vis diffuse reflectance spectroscopy and photoluminescence spectroscopy (PL). They confirmed shift in band gap from UV to visible region and reported that the prepared photocatalyst give better charge separation because of CNTs electrical properties with large surface area as compared to ZnO, Cu-doped ZnO and ZnO/CNTs composite. They used the Cu-doped ZnO/CNTs photocatalyst for the degradation of methyl orange under visible light irradiation and claimed that the prepared photocatalyst results in better photocatalytic degradation as compared to ZnO, Cu-doped ZnO, and ZnO/CNTs composite. Monitoring of COD before and after photo catalysis process showed a marked decrease in COD, which prove the complete oxidation of organic compound along with color removal.

Sahal and Djaja [57] synthesized Fe doped ZnO nanoparticles, and used it for the degradation of methylene blue and methyl orange in the presence of UV-visible light. The prepared sample were characterized by XRD, EDX, SEM, UV-Vis DRS, ESR and vibrating sample magnetometer techniques. They optimized the various parameters like pH, catalyst dosage, scavengers, initial dye concentration and photoactive species. Spin magnetization of Fe^{+2} was found greater than Fe^{+3}that resulted in the degradation of both dyes by Fe^{+2}-doped ZnO is more effective than Fe^{+3}.

Mahn B.Nguyen, Giang H. Le et al. [58] synthesized the Ag/Zn-BTC/GO composites (BTC: benzene-1, 3, 5-

tricarboxylic, GO: graphene oxide) with different Ag/Zn molar ratios were synthesized using microwave-assisted hydrothermal treatment. The Ag/Zn-BTC/GO composites showed the excellent photocatalytic performance in the reactive yellow 145 dye (RY-145) degradation under irradiation of visible light with nearly 100% of RY-145 removal after 35 min, as compared to Zn-BTC/GO and Ag-BTC/GO. The effect of catalyst dosage, pH and dye concentration on the efficiency of photocatalytic activity of bimetallic Ag_{50}-Zn_{50}-BTC/GO was also noted. The improvement in photocatalytic activity of bimetallic Ag-Zn-BTC/GO could be given by the synergism of (i) absorption of visible light confirmed by UV-Vis diffuse reflectance spectra; (ii) the increased lifetime as evidenced by photoluminescence spectra and transient photocurrent response; (iii) the increased oxygen vacancy defects as confirmed by X-ray photoelectron spectroscopy results. The degradation pathway of RY-145 dye was also predicted based on liquid chromatography-mass spectrometer analysis. The removed chemical oxygen demand, biological oxygen demand, total organic carbon outcomes indicated the high mineralization ability for RY-145 degradation over Ag-Zn-BTC/GO.

Wenqiang Ding, Liden Zhao, et al.[59] provided the environmental friendly route to fabricate ternary silver/silver oxide/zinc oxide ($Ag/Ag_2O/ZnO$) photocatalyst with assistance of bovine serum albumin (BSA). The structural analysis indicated that $Ag/Ag_2O/ZnO$ photocatalyst was a 3D-flowerlike architecture. Nanoparticles composed of Ag and Ag_2O in diameter about 40 nm attach on the surfaces of ZnO "petals" and form a heterojunction structure with ZnO. The ultraviolet-visible (UV–vis) spectra and photoluminescence

(PL) spectra showed that the obtained $Ag/Ag_2O/ZnO$ nanocomposite displayed an enhanced visible-light absorption and a decreased fluorescence emission compared to that of ZnO. The photocatalytic performance of $Ag/Ag_2O/ZnO$ nanocomposite was evaluated by photocatalytic degradation of methylene blue (MB) under simulated visible light irradiation. The results indicated that $Ag/Ag_2O/ZnO$ nanocomposite exhibited better photocatalytic activity than that of single- and two-component photocatalyst including ZnO, Ag_2O, TiO_2 and Ag/ZnO. $Ag/Ag_2O/ZnO$ nanocomposite also has a good recycling stability and still maintained a high degradation efficiency (85%) after four recycles. The improved photocatalytic activity was credited to the synergistic effect of Ag, Ag_2O and ZnO nanophases in the $Ag/Ag_2O/ZnO$ heterojunction, which resulted in an effective charge separation and a low recombination of photo-induced electron-hole pairs.

CHAPTER THREE

THEORIES OF CHARACTERIZATION TECHNIQUES

Ezza Zulfiqar

Centre for Applied Chemistry, Institute of Chemistry, Punjab University Lahore, Pakistan

***Corresponding: ezzazulfiqar14@gmail.com**

Abstract

Different characterization techniques were used for analysis of bimetallic NPs. Fourier transform infrared
spectroscopy (FT-IR) and Ultra-Violet/Visible spectroscopy are used here for morphological and structural characterization. Fourier transform infrared spectroscopy (FT-IR) is used for structural analysis. The dimensional analysis of metal nanoparticles for photocatalytic degradation of dye under different conditions were done by help of UV-Visible spectroscopy.

1. Fourier Transform Infra-red (FT-IR) spectroscopy

Fourier Transform Infra-red spectroscopy usually referred as FT-IR. Electromagnetic radiation of wavelength between 4000 and 400cm-1 interact with matter these radiations are known as IR radiation and its application to chemistry is called FT-IR spectroscopy. FT-IR spectroscopy due to its unique features is the most widely used method among all other methods of infrared spectroscopy for the qualitative analysis of different substances. FT-IR spectroscopy is used to obtain fingerprints of compound, for the detection of functional groups, for determination of consistency of the materials

1.1 Major regions of FT-IR spectrum

There are usually three infrared regions near IR Region, mid IR Region, far IR Region.

1. Near IR Region: Very high energy region round about 14000-4000 cm-1 (wavelength 0.8-2.5 um). This region can excite overtone and harmonic vibrations.

2. Mid IR Region: Mid IR Region range approximately from 4000-400 cm-1 (2.5- 25 um). This region may be used to study the fundamental vibrations and associated rotational vibrational structure.

3. Far IR Region: This low energy region in range of 400-10 cm-1 (25-1000 um) used for rotational spectroscopy.

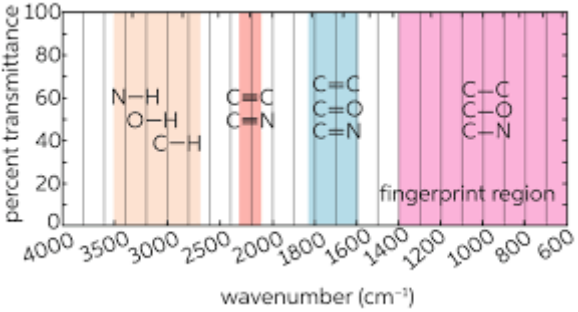

Figure 1: *Regions of infrared spectroscopy*

1.2 Theory of FT-IR Spectroscopy

FT-IR Spectroscopy is used to obtain IR spectra and that spectrum formed due to alternation in rotational and vibrational level of molecules. The radiation having energy below 100cm-1 can induce the electronic transitions while radiations with energy 10,000-100cm-1 are required for causing the vibrational transition in any molecule. These transitions appear in the form of discrete lines because energy levels are quantized. A molecule facing IR radiations should have changed in their dipole moment. There are basically two kinds of vibrational mode i-e stretching vibrations and bending vibrations. Stretching involves movement of atoms in such a way that cause change in bond length, movement can be symmetrical or anti symmetrical stretching. Bending vibrations cause change in bond angles. Bending vibrations are of four types two are in plane and two are out of plane i.e. rocking, scissoring, twisting and wagging shown in figure 2.

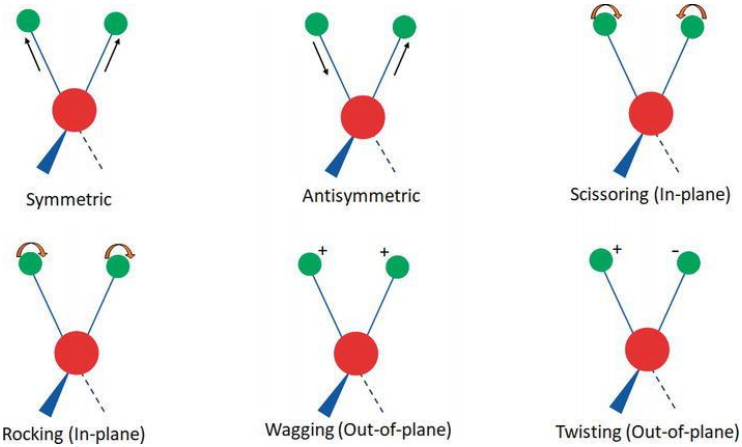

***Figure 2**: Vibrational modes of IR spectroscopy*

1.3 Instrumentation

There are four important parts in FT-IR which are described as follow and diagrammatical representation of FT-IR is shown in figure 3.3.

Source From glowing black body source IR radiations emitted. The amount of energy is controlled by aperture used when radiation passed through it.

Interferometer FT-IR most essential part is Michelson interferometer. Beam is entered through beam splitter which divides the beam into two equal parts. One part of beam goes to stationary mirror while other beam moves to the moving mirror. Both beams of different path length are reflected back and constructive and destructive

Sample Combined beam coming from the interferometer entered into sample compartment. Here in sample compartment beam can be transmitted or reflected depending on type of sample analysis being accomplished.

Detector Beam finally passed through the detector for final measurement. The detectors used are specifically designed to measure interferometer signal resulting from the combination of the bond frequency with specific IR radiations.

The Computer In computer measured signals converted to digitized signal via mathematical operation Fourier transform. The final infrared spectrum is passed to the user for any further interpretation and manipulation.

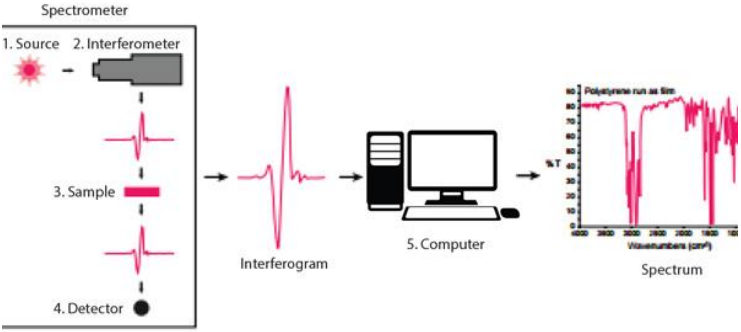

Figure 3: *Instrumentation of FT-IR*

FT-IR as shown in figure 3 is preferably used over older IR techniques because of several reasons like it is simple mechanically because of only one moving part, it is non-destructive techniques, it is sensitive than dispersive IR spectrophotometer and it gives precise measurement methods which requires no calibration.

1.4. Application of FT-IR Spectroscopy

Applications of FT-IR spectroscopy are as follow.

1. Both quantitative and quantitative analysis of an analyte in a sample can be provided by this technique.
2. FT-IR is preferably used for the determination of structure of compound by interpretation and correlation of IR spectra. 3.

FT-IR spectroscopy is applicable for detection of enantiomers having same physical properties.

4. FT-IR technique is useful for environment study by monitoring air and water quality.

5. FT-IR spectroscopy is also useful in forensics and food.

6. Without this technique it is impossible to achieve the characterization or quantitative measures of the analytes in samples in the field of chemistry, biochemistry, biotechnology etc.

2. Ultraviolet-Visible (UV-Vis) spectroscopy

Interaction of electromagnetic radiations with molecular species is called spectroscopy. UV/Visible spectroscopy is a type of absorption spectroscopy and exists between the infrared and visible region. Range of UV/Visible is extending from 100-400 nm in wavelength. UV/Visible region further divided into a far ultraviolet region (vacuum ultraviolet region) and near ultraviolet region. Due to some impurities like oxygen absorbed in this region it's equipped with vacuum pump so that's why far ultraviolet region can also be called as vacuum ultraviolet region. Wavelength Ranges of Far ultraviolet region are 10-200 nm and near ultraviolet region 200-400 nm. In this UV/Visible region atoms and molecules undergo transition from ground state to excited state.

2.1. Principle

UV-Visible spectroscopy follows Beer-lambert law. Beer-lambert law is a relationship between the absorbance, concentration and path length of cell used. This law based on two statements, one given by Lambert and other by Beer. According to lambert statement, the absorbance of monochromatic light passing through a solution of absorbing substance increase when path length of cell used increases. And

Beer states that, the absorbance of monochromatic light passing through solution remains constant if the concentration of absorbing specie present in that solution is constant. The absorbance of radiation by analyte is directly proportional to concentration of absorbing specie present in that solution is constant. The absorbance of radiation by analyte is directly proportional to concentration of that species and path length of the cell.

$$A \alpha l \quad (2.1)$$

$$A \alpha c \quad (2.2)$$

From equation 2.1 and 2.2

$$A \alpha l c \quad (2.3)$$

$$A = \varepsilon l c \quad (2.4)$$

From absorbance and transmittance relation we know that absorbance equal to

$$A = \log I_o/I \quad (2.5)$$

$$\varepsilon cl = \log I_o/I \quad (2.6)$$

Here ε is molar absorptivity, C is molar concentration of solute, Io is intensity of light fall on sample cell, and I is light intensity leaving the sample cell. This law is not always applicable due to many reasons like sometime association occur, polymerization occur, or molecules may be dissociated and due to coagulation of solvent molecules and solute molecules.

2.2. Instrumentation

Generally, UV-Visible spectrophotometer consists of Irradiation source, monochromator, beam splitter, reference cell, sample cell, prism, detector amplifier and recorder.

Irradiation source in spectrophotometer tungsten filament generally employed as the source of radiation for the Vis region. On the other hand, Deuterium lamps or Hydrogen

discharge lamps are normally employed for the UV region radiations because of its whole range covering properties.

Monochromator gives the function of choosing the wavelength from the UV-Visible region into its components on the other hand the exit slit controls the radiation output.

Beam splitter Advanced double-beam spectrophotometer contains the beam splitter that splits the existing radiation into two beams. One beam is allowed to pass through sample while other is passed through the reference cell.

Sample cell the cell usually used is of mostly quartz. Although cell made up of glass can be used but due to limitation that it cannot be applicable in UV-region it is preferred. The sample is placed in the quartz cuvette and then are further placed in the path of the beam coming from the monochromator.

Detectors For the determination of sample absorbance phototubes and photomultiplier are mostly used. Photomultiplier detectors are generally employed in a double-beam spectrophotometer. This detector is more suitable and accurate as compared to other phototubes detectors used previously.

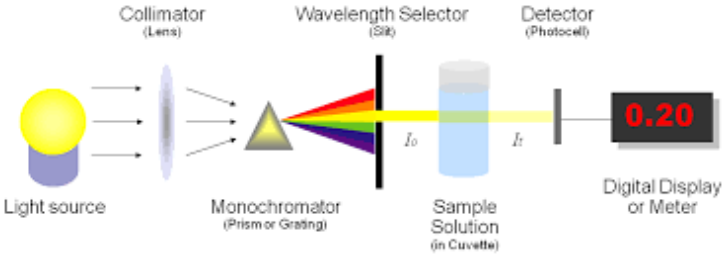

Figure 4: *Schematic representation of UV-Visible spectrophotometer*

2.3 Applications

The applications of UV-Visible spectroscopy are as follow.

1. For structural determination this technique is applicable.
2. Quantitative analysis is mostly performed by UV-Visible spectroscopy.
3. For detection of impurities UV-Visible spectroscopy usually preferred.
4. UV-Visible spectroscopy also used for qualitative determination of colored compounds and metals.
5. For physical parameters like dissociation constants linked to acid and bases can also be evaluated using UV-Visible spectroscopy.
6. In certain compounds stereo chemical details can be provided by this technique.
7. UV-Visible spectroscopy is used for reaction rate determination which involves change in an absorbing group.

CHAPTER FOUR

MATERIALS AND METHODS

Ezza Zulfiqar
Centre for Applied Chemistry, Institute of Chemistry, Punjab University Lahore, Pakistan

***Corresponding:** ezzazulfiqar14@gmail.com

1. Apparatus used

1. Hot plate
2. Magnetic stirrer
3. Beakers (100, 250, 500ml)
4. Conical flask
5. Pipette
6. Filter paper
7. Round bottom flask
8. Weighing balance
9. Glass vials
10. Furnace
11. Oven
12. Autoclave
13. Calciner

Most of the apparatus used was purchased from Pyrex England and it was rinsed with distilled water and dried properly before use.

2. Chemicals used

1. Metal salts i.e. Silver nitrate [$AgNO_3$]
2. Zinc nitrate hexahydrate [$ZnNO_3(H_2O)_6$
3. Copper sulphate hexahydrate [$CuSO_4(H_2O)_6$]
4. Cetyltrimethylammoniumbromate[CTAB]
5. Thiourea[H_2NCSNH_2]
6. Sodium borohydride [$NaBH_4$]
7. Methylene Blue

3. Methods

3.1. Preparation of stock solutions

Preparation of 0.6M Cu(SO4).6H2O

To prepare 1M Cu(SO4).6H2O **2.0592g** of salt was taken and dissolved in 50ml of distilled water according to the given formula.

Molarity (M) = Mass of solute (g)/Molar mass of solute (g/mol) x volume of solution (L)

Preparation of 0.6M Thiourea

To prepare 0.6M Thiourea (H2NSHNH2) **0.9163g** of it was taken and dissolved in 50ml of distilled water.

Preparation of 0.01M Zn(NO3).6H2O

To prepare 0.01M Zn(NO3).6H2O **0.14g** of the salt was taken in a beaker and dissolved in 50ml of distilled water.

Preparation of 0.01M AgNO3

To prepare 0.01M AgNO3 **0.025g** of salt was taken and dissolved in 15ml of distilled water.

Preparation of 0.01M NaBH4

To prepare 0.01M of sodium borohydride **0.01g** of it was taken in a beaker and dissolved it in 50ml of distilled water.

3.2 Preparation of bimetallic nanoparticles

A solution of CuSO4 (H2O)6 [50ml,0.6M] was added to the solution of surfactant CTAB (0.3g) under stirring. Then, 50ml ofH2NCSNH2 (0.6M) was added to the above solution under vigorous stirring. The mixture was located in an autoclave, heated, and kept at 160℃ for 4 hours. After cooling process, the product was washed, dried in vacuum oven at 70℃ for 12 hours and calcined at 450℃ for 90 minutes. The CuS nanoparticles (0.02g) was dispersed in 100ml of deionized water. At dark conditions, ZnNO3 (15ml of 0.01M) and AgNO3 (15ml of 0.01) solution was added drop by drop to above suspension. Then, ice cold sodium borohydride (20ml, 0.01M) was augmented and stirred for 30 minutes. The solid was dried at 70℃ and calcined at for 90 min.

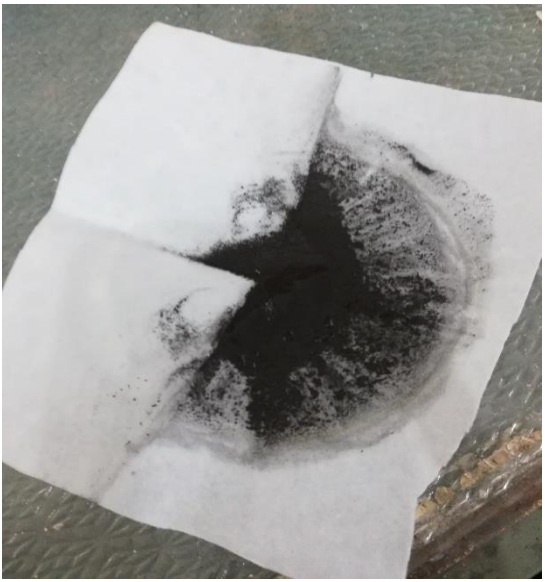

Figure 1: *Air drying of bimetallic nanoparticles*

3.3 Photocatalysis of Methylene Blue (MB)

Solution preparation

First of all, 1000ppm solution of MB was prepared by dissolving 1g of MB in 1 liter flask and then diluting it up to the mark. This was our stock solution. From this standard solutions of 5, 10, 15, 20, 25, 30 ppm were prepared by dilution method. The λmax (665 nm) of solutions were found and absorbance of each solution was noted down. Calibration line was plotted between the concentration and absorbance of standard solution.15 ppm solution was selected for further procedure.3.75ml of 1000ppm solution was transferred to 250 ml and made it up to the mark to make 15 ppm concentration of dye solution.

Figure 2: *Solutions of different concentrations of MB*

3.4. Effect of different Parameters

1. In the absence of sun light to achieve equilibrium

50ml of 15 ppm solution of MB was taken along with 1g of bimetallic Zn/Ag nanoparticles in a round bottom flask and magnetic stirring of solution was carried out in the dark environment to achieve equilibrium before irradiation treatment.

2. In the presence of sun light

After that, the solution of MB was stirred in the presence of sunlight without any catalyst for about 1 hour to gain equilibrium for adsorption and desorption.

3. with different concentrations of catalyst

Then, the different concentration of bimetallic catalyst i.e. 0.05, 0.1, 0.15, 0.2 0.25, 0.3mg, were added to the MB solution and stirred for 30 minutes each solution respectively in the presence of sun light. The characteristic peak of each solution by UV-visible spectroscopy shows the %age degradation of each solution. It was shown that the solution with 0.2

concentration of bimetallic nanoparticles showed the highest degradation of dye.

4. At different time intervals

After that, the 50ml of solution with 0.2mg concentration of catalyst that showed the greatest degradation was taken and stirred in the sunlight. From this, the 10 ml of solution was taken in quartz cell after every 20 min for UV-visible spectroscopy. Spectra through double beamed UV-visible spectrophotometer were measured within the range of 200-800nm and the variations in the peaks were noted.

Figure 3: *Degradation in the absence of sun light*

Figure 4: *Photocatalytic Degradation*

3.5. Mechanism

The process starts with the excitation of electrons into the conduction band of Zn-Ag nanosheets generating holes in the valence band upon sunlight exposure. These photogenerated holes interact with water to generate hydroxyl radicals (.OH), while the photogenerated electrons interact with oxygen molecules to form superoxide radicals (.O)$_2$. Reactions of these formed organic dye molecules result in their degradation and formation of products such as CO2 and H2O. These processes are described by the following equations.

Bimetallic catalyst (Zn/Ag) + $h\nu \rightarrow e^-$(C.B) + h^+(V.B)

$$e^- + .O_2 \rightarrow \bullet O_2^-$$

$$h^+ + OH^- \rightarrow .OH$$

$$h^+ + H_2O \rightarrow H^+ + .OH$$

$$.OH + MB \rightarrow \text{Degradation}$$

$$.O_2^- + MB \rightarrow \text{Degradation}$$

For better understanding, the process of photocatalytic degradation is shown in the figure given below.

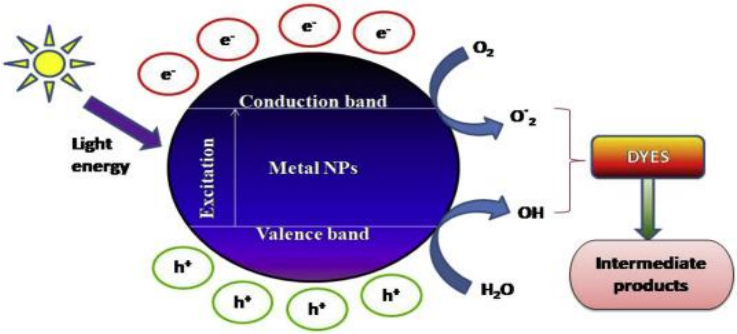

Figure 5: *Mechanism of Photocatalytic degradation*

4. CHARACTERIZATION

4.1 Fourier Transform Infra-red spectroscopy

Perkin Elmer, RX 1 FT-IR spectrometer was employed to evaluate the FT-IR spectra of samples to judge the peak patterns of CuS nanoparticles formed for the synthesis of bimetallic Ag-Zn, which was used as coating material. For this, 10ml of sample was taken in glass vial and oven dried. The resultant spectrum of solid was obtained in near infrared region (4000 to 650 cm^{-1}) and was further interpreted as for defining structural moieties. FT-IR Perkin Elmer spectrometer is shown in Figure 6.

Figure 6: *FT-IR Spectrometer Instrument*

4.2 UV-Visible spectroscopy

UV-Visible analysis was utilized for monitoring reaction progress because both reactant and products are UV active. The confirmation of synthesis of CuS, Ag-Zn bimetallic was made by Labmoed, Inc. UVD-3500, double beam Ultra-Violet spectrophotometer. Also, the degradation of MB dye was also indicated by this instrument. The absorption peaks were identified to govern the values of λmax for different reactions within the range of 200-800 nm and is shown in Figure 7.

Figure 7: UV-visible spectrometer

CHAPTER FIVE

RESULTS AND DISCUSSION

Ezza Zulfiqar

Centre for Applied Chemistry, Institute of Chemistry, Punjab University Lahore, Pakistan

***Corresponding: ezzazulfiqar14@gmail.com**

1. UV analysis of CuS nanoparticles

Synthesis of CuS nanoparticles used as coating foe bimetallic synthesis by hydrothermal method was confirmed by visual observation on the basis of color developed during the course of reaction as well as by the formation of suspension. Metal nanoparticles when interact with an exciting light of comparable size, show optical absorption band in UV-VIS region. This property of metal nanoparticles is termed as surface Plasmon resonance (SPR). It also confirms the formation of nanoparticles. The degree of reduction of metal salt to metal nanoparticle is interpreted by change in the intensity of color on addition of surfactant. The SPR CuS produced a peak centered near 360nm. The SPR peak thus obtained is sensitive not only to nature, concentration, size and shape of nanoparticles but also depends upon their inner particle distance and surrounding medium. It was observed that the reduction of Copper Sulphate to CuS nanoparticles started at the beginning of the reaction and completed at almost two minutes at room temperature indicating rapid synthesis of CuS nanoparticles. It is reported in literature that typical CuS nanoparticles show the characteristic SPR in the range of 250-800nm. Figure 1 exhibits the SPR wavelength peak at 360nm verifying the presence of CuS nanoparticles in the solution.

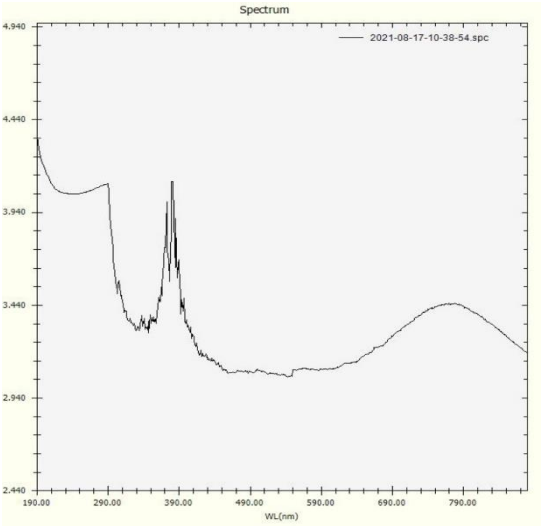

Figure 1: *Verifying the presence of CuS nanoparticles in the solution*

2. UV analysis of Zn-Ag bimetallic nanoparticles

Synthesis of bimetallic Zn-Ag bimetallic nanoparticles by hydrothermal method was confirmed by the UV analysis of nanoparticles. The SRP Zn-Ag bimetallic nanoparticles produced a peak near 240 nm. The nanoparticles were produced by using reducing agent i.e. NaBH4. In literature studies shows the peak of ZnO and Ag separately in the range of 300-360nm. The bimetallic consists of the mixture of more metals that showed the peak at 240nm. Figure 2 shows the SRP peak at 240nm that shows the presence of bimetallic nanoparticles.

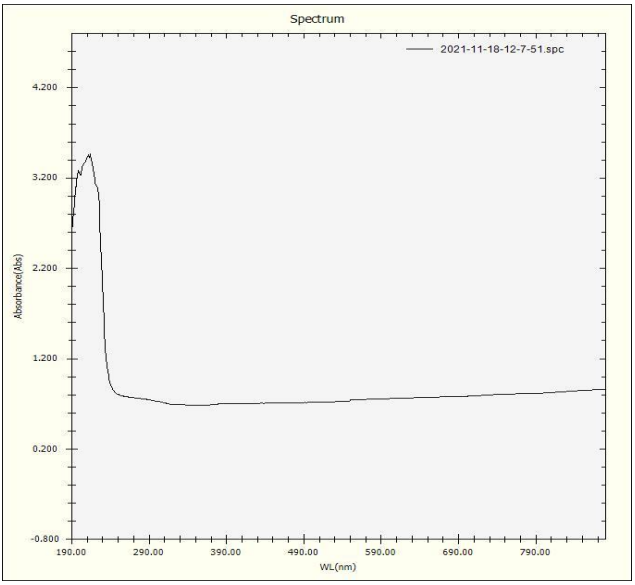

***Figure 2**: SRP peak at 240nm that shows the presence of bimetallic nanoparticles*

3. FT-IR analysis of CuS nanoparticles

FTIR analysis is employed as a confirmatory technique to the formation of nanoparticles. It provides an impression to the rotational and vibrational modes of the existing molecules and consequently it helps to identify the functional phytochemical constituents that are involved in the reduction and stabilization of nanoparticles produced i.e. CuS-NPs. The peak of 344029 cm^- shows the presence of O-H bond. The peak at 2922cm^- shows C-H bond. While the peak at 2854cm^- shows the CuS molecule. The peak at 1635cm^-, 1425cm^-, 1280cm^- shows the weak bending frequency of C=C, C-H, and C-C respectively.

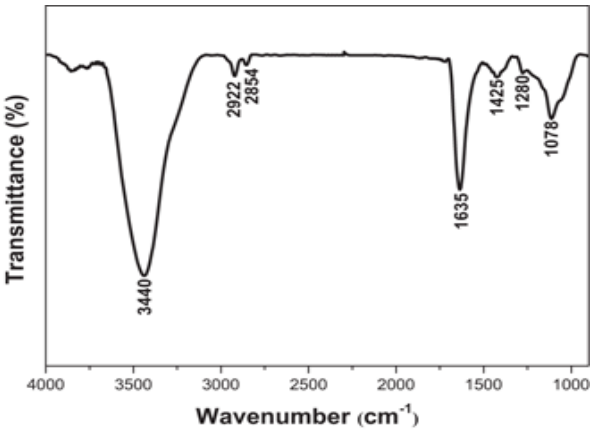

Figure 3: *FT-IR analysis of CuS*

4. FT-IR of ZnO-Ag bimetallic nanoparticles

The FT-IR of ZnO-Ag bimetallic is shown in figure 5.2. A peak at 500 cm^{-} shows the characteristic ZnO-Ag nanoparticles. The peak at 3500 cm^{-} show the strong stretching vibrations of OH group. While the peaks at 1500 cm^{-} shows the weak vibrations of OH group

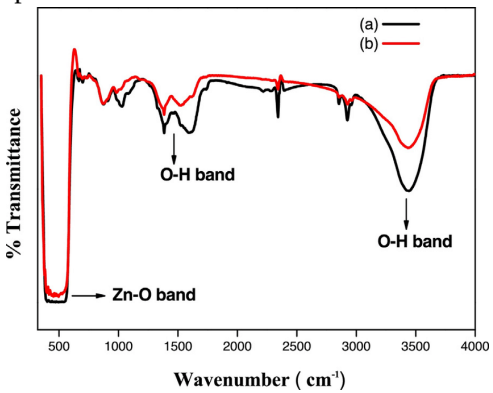

Figure 4: *Black line shows the ZnO and red line shows the Ag nanoparticles*

5. Photocatalytic degradation of MB in the absence of catalyst

The concentrations of different solutions of MB were stirred in the absence of catalyst at different time of intervals and the sample were studied by using UV spectroscopy. The graph shows the peak at 650nm which is the λmax for MB in the literature. The peak of MB lowers down as we move to the left of graph which shows the rapid degradation of MB. The peak at 210 and 300 nm shows the formation of CO2 and H2O as MB degraded into CO2 and H2O. The graph as shown in fig. 5.5 shows the degradation at different intervals of time. As the time increases, the absorption increase. The maximum absorption by the MB solution is at 40 minutes. The degradation curves are also given in the graph.

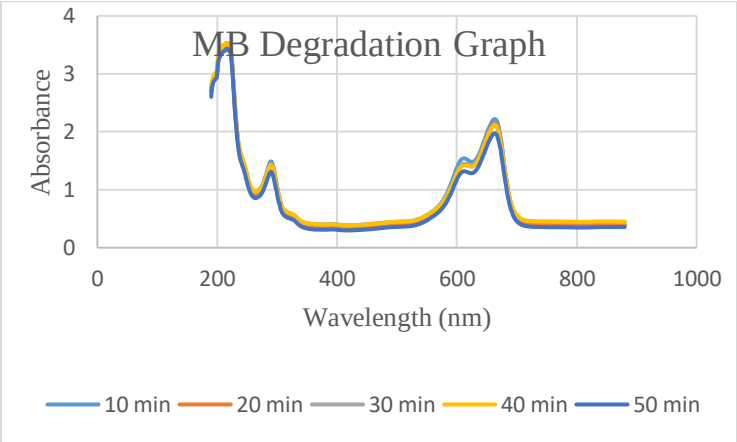

Figure 5: *Degradation curve in the absence of catalyst*

6. Photocatalytic degradation in the presence of catalyst

The degradation of MB was studied in the presence of sunlight with the different concentrations of catalysts with the same interval of time. The best degradation curve was shown by the

solution with 0.2g catalyst. Then, with this solution the degradation was studied at different intervals of time. The MB showed the rapid degradation with few seconds contact time of catalyst i.e. broad peak at 650nm that is of MB which means that MB has been degraded to much extent. The maximum degradation is at 10 minutes of interval. As the time increases, the absorption of MB increases which shows the less degradation as compare to the graph line showing greater absorption. The peak of 230 nm shows the presence of bimetallic catalyst.

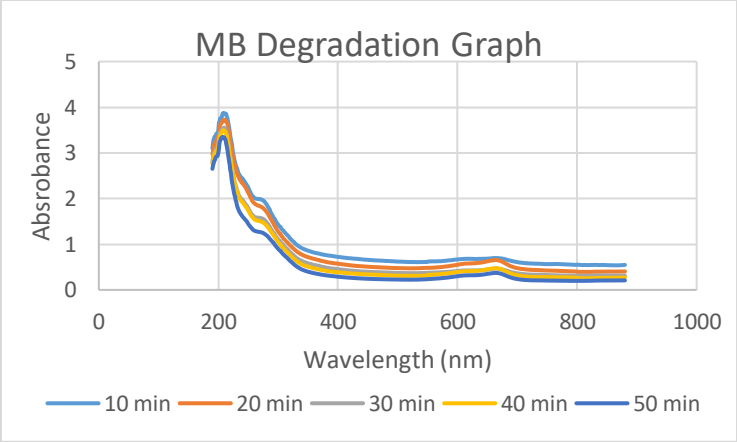

Figure 6: *Photocatalytic degradation in the presence of catalyst*

References

1. Qi, J., et al., Multi-shelled CeO 2 hollow microspheres as superior photocatalysts for water oxidation. Nanoscale, 2014. **6**(8): p. 4072-4077.
2. Paul, A. and S.S. Dhar, Designing Cu2V2O7/CoFe2O4/g-C3N4 ternary nanocomposite: A high performance magnetically recyclable photocatalyst in the reduction of 4-nitrophenol to 4-aminophenol. Journal of Solid State Chemistry, 2020. **290**: p. 121563.
3. Fu, Y., et al., High photocatalytic activity of magnetically separable manganese ferrite–graphene heteroarchitectures. Industrial & engineering chemistry research, 2012. **51**(2): p. 725-731.
4. Eshaq, G. and A.E. ElMetwally, Bmim [OAc]-Cu2O/g-C3N4 as a multi-function catalyst for sonophotocatalytic degradation of methylene blue. Ultrasonics sonochemistry, 2019. **53**: p. 99-109.
5. Mosbah, A., et al., Peptides Fixing Industrial Textile Dyes: A New Biochemical Method in Wastewater Treatment. Journal of Chemistry, 2019. **2019**.
6. Kumar, P.S., S.J. Varjani, and S. Suganya, Treatment of dye wastewater using an ultrasonic aided nanoparticle stacked activated carbon: kinetic and isotherm modelling. Bioresource technology, 2018. **250**: p. 716-722.
7. Katheresan, V., J. Kansedo, and S.Y. Lau, Efficiency of various recent wastewater dye removal methods: A review. Journal of environmental chemical engineering, 2018. **6**(4): p. 4676-4697.
8. Yagub, M., et al., Dye and its removal from aqueous solution by adsorption: a review. Adv Colloid Interfac 209: 172–184. 2014, ed.
9. Vakili, M., et al., Application of chitosan and its derivatives as adsorbents for dye removal from water and wastewater: A review. Carbohydrate polymers, 2014. **113**: p. 115-130.
10. Burgess, R., Harvesting color: How to find plants and make natural dyes. 2011: Artisan Books.

11. Salim, A.S., Literature in dyes for industrial fields. International Journal of Chem-informatics Research, 2019. **5**(1): p. 36-40.
12. Booth, G., et al., Dyes, general survey. Ullmann's Encyclopedia of Industrial Chemistry, 2000.
13. Mirsalari, S.A. and A. Nezamzadeh-Ejhieh, The catalytic activity of the coupled CdS-AgBr nanoparticles: a brief study on characterization and its photo-decolorization activity towards methylene blue. Desal. Water Treat, 2020. **175**: p. 263-272.
14. Yang, Z.-Y., Kinetics and mechanism of the adsorption of methylene blue onto ACFs. Journal of China University of Mining and Technology, 2008. **18**(3): p. 437-440.
15. Raffatulah, M., et al., Adsorption of methylene blue on low-cost adsorbent: a review. J. Chem. Eng, 2010. **177**: p. 7080.
16. Matthews, R.W., Photooxidative degradation of coloured organics in water using supported catalysts. TiO2 on sand. Water research, 1991. **25**(10): p. 1169-1176.
17. Sharma, A., et al., Photocatalytic reactions of xylidine ponceau on semiconducting zinc oxide powder. Journal of Photochemistry and Photobiology A: Chemistry, 1995. **86**(1-3): p. 197-200.
18. Sakthivel, S., et al., Solar photocatalytic degradation of azo dye: comparison of photocatalytic efficiency of ZnO and TiO2. Solar energy materials and solar cells, 2003. **77**(1): p. 65-82.
19. Shen, W., et al., Photocatalytic degradation for methylene blue using zinc oxide prepared by codeposition and sol–gel methods. Journal of Hazardous Materials, 2008. **152**(1): p. 172-175.
20. Poulios, I. and I. Tsachpinis, Photodegradation of the textile dye Reactive Black 5 in the presence of semiconducting oxides. Journal of Chemical Technology & Biotechnology: International Research in Process, Environmental & Clean Technology, 1999. **74**(4): p. 349-357.
21. Srinivas, P.R., et al., Nanotechnology research: applications in nutritional sciences. The journal of nutrition, 2010. **140**(1): p. 119-124.

22. Scheu, M., et al., Mapping nanotechnology patents: The EPO approach. World Patent Information, 2006. **28**(3): p. 204-211.
23. Kung, H.H. and M.C. Kung, Nanotechnology: applications and potentials for heterogeneous catalysis. Catalysis today, 2004. **97**(4): p. 219-224.
24. Noguez, C., Surface plasmons on metal nanoparticles: the influence of shape and physical environment. The Journal of Physical Chemistry C, 2007. **111**(10): p. 3806-3819.
25. Hanke, T., et al., Tailoring spatiotemporal light confinement in single plasmonic nanoantennas. Nano letters, 2012. **12**(2): p. 992-996.
26. Kelly, K.L., et al., The optical properties of metal nanoparticles: the influence of size, shape, and dielectric environment. 2003, ACS Publications. p. 668-677.
27. Farooqi, Z.H., et al., Engineering of silver nanoparticle fabricated poly (N-isopropylacrylamide-co-acrylic acid) microgels for rapid catalytic reduction of nitrobenzene. Journal of Polymer Engineering, 2016. **36**(1): p. 87-96.
28. Vatta, L.L., R.D. Sanderson, and K.R. Koch, Magnetic nanoparticles: Properties and potential applications. Pure and applied chemistry, 2006. **78**(9): p. 1793-1801.
29. Seo, Y.S., et al., Catalytic reduction of 4-nitrophenol with gold nanoparticles synthesized by caffeic acid. Nanoscale research letters, 2017. **12**(1): p. 1-11.
30. Ansar, S.M. and C.L. Kitchens, Impact of gold nanoparticle stabilizing ligands on the colloidal catalytic reduction of 4-nitrophenol. ACS Catalysis, 2016. **6**(8): p. 5553-5560.
31. Li, J., C.-y. Liu, and Y. Liu, Au/graphene hydrogel: synthesis, characterization and its use for catalytic reduction of 4-nitrophenol. Journal of Materials Chemistry, 2012. **22**(17): p. 8426-8430.
32. Parveen, R. and G. Tremiliosi-Filho, A step ahead towards the green synthesis of monodisperse gold nanoparticles: the use of crude glycerol as a greener and low-cost reducing agent. RSC advances, 2016. **6**(97): p. 95210-95219.
33. Zeng, T., et al., In situ growth of gold nanoparticles onto polydopamine-encapsulated magnetic microspheres for

catalytic reduction of nitrobenzene. Applied Catalysis B: Environmental, 2013. **134**: p. 26-33.
34. Choi, K., T. Kang, and S.-G. Oh, Preparation of disk shaped ZnO particles using surfactant and their PL properties. Materials Letters, 2012. **75**: p. 240-243.
35. Gharoy Ahangar, E., et al., Preparation and characterization of PVA/ZnO nanocomposite. Journal of Food Processing and Preservation, 2015. **39**(6): p. 1442-1451.
36. Al-Fori, M., et al., Antifouling properties of zinc oxide nanorod coatings. Biofouling, 2014. **30**(7): p. 871-882.
37. Liang, S., et al., A novel ZnO nanoparticle blended polyvinylidene fluoride membrane for anti-irreversible fouling. Journal of membrane science, 2012. **394**: p. 184-192.
38. Bian, W., et al., The intermediate products in the degradation of 4-chlorophenol by pulsed high voltage discharge in water. Journal of hazardous materials, 2011. **192**(3): p. 1330-1339.
39. Ponce, A.A. and K.J. Klabunde, Chemical and catalytic activity of copper nanoparticles prepared via metal vapor synthesis. Journal of Molecular Catalysis A: Chemical, 2005. **225**(1): p. 1-6.
40. Xiong, J., et al., Synthesis of highly stable dispersions of nanosized copper particles using L-ascorbic acid. Green Chemistry, 2011. **13**(4): p. 900-904.
41. Kim, Y.H., et al., Synthesis of Cu nanoparticles prepared by using thermal decomposition of Cu-oleate complex. Molecular Crystals and Liquid Crystals, 2006. **445**(1): p. 231/[521]-238/[528].
42. Zhang, Q.-l., et al., Preparation of copper nanoparticles by chemical reduction method using potassium borohydride. Transactions of Nonferrous Metals Society of China, 2010. **20**: p. s240-s244.
43. Reverberi, A.P., et al., Synthesis of copper nanoparticles in ethylene glycol by chemical reduction with vanadium (+ 2) salts. Materials, 2016. **9**(10): p. 809.
44. Bhanja, S.K., et al., Green synthesis of Ag@ Au bimetallic composite nanoparticles using a polysaccharide extracted from Ramaria botrytis mushroom and performance in catalytic reduction of 4-nitrophenol and antioxidant,

antibacterial activity. Environmental Nanotechnology, Monitoring & Management, 2020. **14**: p. 100341.
45. Zaleska-Medynska, A., et al., Noble metal-based bimetallic nanoparticles: the effect of the structure on the optical, catalytic and photocatalytic properties. Advances in colloid and interface science, 2016. **229**: p. 80-107.
46. Rajbongshi, B., et al., Synthesis and characterization of plasmonic visible active Ag/ZnO photocatalyst. Journal of Materials Science: Materials in Electronics, 2014. **25**(7): p. 2969-2973.
47. Sorbiun, M., et al., Biosynthesis of Ag, ZnO and bimetallic Ag/ZnO alloy nanoparticles by aqueous extract of oak fruit hull (Jaft) and investigation of photocatalytic activity of ZnO and bimetallic Ag/ZnO for degradation of basic violet 3 dye. Journal of Materials Science: Materials in Electronics, 2018. **29**(4): p. 2806-2814.
48. Chen, Y.-C., et al., Facile procedure to synthesize highly crystalline Ag/NiO nanocomposite microspheres and their photocatalytic activity. Journal of Materials Science: Materials in Electronics, 2012. **23**(8): p. 1592-1598.
49. Rycenga, M., et al., Controlling the synthesis and assembly of silver nanostructures for plasmonic applications. Chemical reviews, 2011. **111**(6): p. 3669-3712.
50. Vaiano, V., et al., Enhanced photocatalytic removal of phenol from aqueous solutions using ZnO modified with Ag. Applied Catalysis B: Environmental, 2018. **225**: p. 197-206.
51. Ma, X., et al., Comparison of photocatalytic reaction-induced selective corrosion with photocorrosion: Impact on morphology and stability of Ag-ZnO. Applied Catalysis B: Environmental, 2017. **201**: p. 348-358.
52. Georgekutty, R., M.K. Seery, and S.C. Pillai, A highly efficient Ag-ZnO photocatalyst: synthesis, properties, and mechanism. The Journal of Physical Chemistry C, 2008. **112**(35): p. 13563-13570.
53. Bechambi, O., et al., Photocatalytic activity of ZnO doped with Ag on the degradation of endocrine disrupting under UV irradiation and the investigation of its antibacterial activity. Applied Surface Science, 2015. **347**: p. 414-420.

54. Ren, C., et al., Synthesis of Ag/ZnO nanorods array with enhanced photocatalytic performance. Journal of hazardous materials, 2010. **182**(1-3): p. 123-129.
55. Zhang, X., et al., Shape-dependent localized surface plasmon enhanced photocatalytic effect of ZnO nanorods decorated with Ag. International journal of hydrogen energy, 2014. **39**(16): p. 8238-8245.
56. Ahmad, M., et al., Enhancement in visible light-responsive photocatalytic activity by embedding Cu-doped ZnO nanoparticles on multi-walled carbon nanotubes. Applied surface science, 2013. **285**: p. 702-712.
57. Saleh, R. and N.F. Djaja, UV light photocatalytic degradation of organic dyes with Fe-doped ZnO nanoparticles. Superlattices and Microstructures, 2014. **74**: p. 217-233.
58. Nguyen, M.B., et al., Bimetallic Ag-Zn-BTC/GO composite as highly efficient photocatalyst in the photocatalytic degradation of reactive yellow 145 dye in water. Journal of Hazardous Materials, 2021. **420**: p. 126560.
59. Ding, W., et al., Bovine serum albumin assisted synthesis of Ag/Ag2O/ZnO photocatalyst with enhanced photocatalytic activity under visible light. Colloids and Surfaces A: Physicochemical and Engineering Aspects, 2019. **568**: p. 131-140.
60. Khatami, M., et al., Applications of green synthesized Ag, ZnO and Ag/ZnO nanoparticles for making clinical antimicrobial wound-healing bandages. Sustainable Chemistry and Pharmacy, 2018. **10**: p. 9-15.